Determination of interatomic interactions in $Ca_{10}(PO_4)_6F_2$ (fluorapatite) from structural and lattice-dynamical data*

L. L. Boyer†
Solid State and Materials Laboratory, Princeton University, Princeton, New Jersey 08540

P. A. Fleury
Bell Laboratories, Murray Hill, New Jersey 07971

(Received 18 October 1973)

In this paper we illustrate a method for determining interatomic interactions in complex ionic crystals by considering specifically a rigid-ion model for fluorapatite. Structural data are the primary input to the model while Raman scattering measurements (reported here) are used to determine seven additional parameters. While point charges are assumed, the values within the PO_4^{-3} group are adjusted to account for covalency and compensate for neglecting dipole terms in the oxygen-ion charge distribution. The computed phonon frequencies are in remarkably good agreement with values obtained from both Raman and infrared measurements.

I. INTRODUCTION

In the previous paper (I)[1] a general method was described for determining interatomic potentials for complex ionic crystals in the rigid-ion approximation. Here we illustrate this method for fluorapatite (FAP), which has the chemical formula $Ca_5(PO_4)_3F$ and contains two formula units or 42 ions per unit cell. This compound is of practical interest because the isomorphous material, hydroxyapatite, obtained by replacing the F^- ions by OH^- ions, is the primary constituent of bones and teeth.[2] Nature does not provide large single crystals of hydroxyapatite and only recently have attempts to grow them been successful.[3,4]

In our model we take the fully ionic values of -1, $+2$, and -3 for the charge of the fluorine, calcium, and phosphate ions, respectively, while the distribution of charge within the phosphate ion is treated as an adjustable parameter. Short-range interactions are included for 20 of the nearest ion pairs. All but six of the short-range parameters are determined from the crystal structure, using static-equilibrium conditions (SEC) and assumptions regarding the similarity of various bonds. Results of Raman scattering measurements, reported here, are used to determine the six short-range parameters and the charge distribution of the PO_4^{-3} group.

From group-theoretical considerations there are 33 Raman active modes expected, of which 31 are observed in the spectrum. The computed frequencies match nicely with the measured values and furthermore predict which two of the Raman lines are due to unresolved double peaks. The computed frequencies are also in very good agreement with infrared measurements.

A brief discussion of the experimental technique and apparatus is presented in Sec. II. The static-equilibrium conditions and their solutions for several different models of FAP are discussed in Sec. III. The dynamics of the free PO_4^{-3} ion is reviewed in Sec. IV to aid in the analysis of their vibrations in the crystal. Results of lattice-dynamical calculations are presented and compared with experiment in Sec. V.

II. EXPERIMENTAL TECHNIQUES AND APPARATUS

The Raman spectra reported here were excited using linearly polarized 5145-Å radiation from an argon-ion laser. Light scattered through an angle of 90° from oriented natural crystals of fluorapatite from Durango, Mexico, was imaged using $f/10$ optics onto the slits of a Spex-1400 double monochrometer. At the exit slit a lens focussed the output onto an EMI-9256-S photomultiplier which was cooled by flowing cold nitrogen gas to reduce the dark current. The photomultiplier output was amplified by a Keithley electrometer and displayed on a strip-chart recorder. No discrimination or photon-counting techniques were required in these experiments. The spectrometer slits were typically open to 200 μm resulting in an instrumental linewidth of ~ 5 cm^{-1}. Under these conditions, 100 mW of laser power produced phonon signals of a few nanoamperes for 1200 V applied to the photomultiplier. This range indicates that fluorapatite is a quite typical material as regards its Raman scattering efficiency. All spectra were obtained with the samples at room temperature.

Proper identification of phonon symmetries requires careful measurement of incident and scattered light polarization relative to the crystal axes. The various spectra shown in Fig. 2 are labeled according to the notation $k_1(\epsilon_1\epsilon_2)k_2$, where the letters to the left and right *outside* the parentheses indicate, respectively, incident and scattered prop-

agation directions, while those on the inside left and right indicate, respectively, the incident and scattered electric-field-polarization directions.

In the $z(yx)y$ geometry appreciable broad-band fluorescence was excited by the incident light. This required the occasional zero suppressions which are indicated in the spectra as step baseline discontinuities. Attempts to excite the Raman spectra using shorter-wavelength argon-laser lines—like 4880 or 4765 Å—resulted in fluorescence even stronger than those shown here.

III. STATIC-EQUILIBRIUM CONDITIONS

The crystal structure of FAP is hexagonal with space-group symmetry $P6_3/m\,(C_{6h}^2)$. Fourteen parameters, two lattice constants (a and c), and 12 internal coordinates are needed to completely specify the structure. These have been determined by x-ray diffraction measurements of Sudarsannan *et al.*[5] and it is their results that we have used in our calculations. We adopt their convention for labeling the various ions in the unit cell. Specifically, there are two identical F ions per unit cell occupying the a sites (Wyckoff notation). Similarly four Ca_I ions occupy e sites, six Ca_{II}, six P, six O_I, and six O_{II} ions occupy h sites, and 12 O_{III} ions occupy i sites.

We assume these ions are point charges with values of -1 for F, $+2$ for Ca_I and Ca_{II}, $-3-4Z_O$ for P, and Z_O for the oxygen ions. Z_O is treated as an adjustable parameter to account for covalency in the PO_4^{-3} groups and at the same time compensate for neglecting dipole terms in the charge distribution of the oxygen ions.

In Table I we list the lengths of 23 of the shortest bonds in FAP and identify each bond with a label denoting its short-range contribution to the potential energy. These energies are labeled ψ if they refer to bonds within a PO_4^{-3} group and otherwise ϕ. The indices identify the bond according to type and relative bond length. For example, $\psi_{OO}(3)$ denotes the short-range energy of the third-shortest oxygen-oxygen bond in the PO_4^{-3} group. Not included in this listing are ϕ_{PX} interactions. These are insignificant since the P ion is relatively small and is only in direct contact with the oxygen ions its own PO_4^{-3} group.

There are 14 independent static-equilibrium conditions (see Paper I[1]) corresponding to the number of crystal structure parameters, which impose constraints on the first derivatives of the short-range energy of these bonds with respect to their lengths (ψ' and ϕ'). The equations are linear in the ψ' and ϕ' parameters and the coefficient matrix is determined from the crystal structure while the Coulomb contribution depends also on Z_O. Two of the equations express external-strain conditions while 12 arise from internal strains. Of the latter 12 equations, none arise from the F ions, one from the Ca_I ions, two each from the ions occupying h sites, and three from the O_{III} ions—corresponding to the number of parameters required to determine the equivalent positions in each case.

If we terminate the short-range interaction after $\phi_{CaO}(6)$ the number of unknown short-range forces is also 14. However, the resultant 14×14 matrix is very nearly singular. The reason for this is that in a perfect PO_4^{-3} tetrahedron the force on one of the oxygens due to P is along the same line as the total force due to the other three oxygens. While the PO_4^{-3} groups in the crystal are not perfect tetrahedra, their approximate tetrahedral coordination causes the nearly singular condition. This difficulty is removed by choosing some value for one of the ψ' parameters and including $\varphi'_{CaO}(7)$ as an unknown. Ultimately the choice is made from lattice-dynamical considerations, and in our calculations we select the value of $\psi'_{OO}(4)$ in this manner.

Given the value of $\psi'_{OO}(4)$ and the charge Z_O the static-equilibrium conditions are easily solved for the short-range forces. The dependence of the

TABLE I. Bond lengths (Å), ion-pair labels of Mackie and Young, and short-range energy labels for the 21 shortest bonds in FAP. Pairs not in the PO_4^{-3} groups but involving P ions are not included.

Bonds within the PO_4^{-3} group			Bonds not in the PO_4^{-3} group					
Ion pair	Bond length	Short-range energy	Ion pair	Bond length	Short-range energy	Ion pair	Bond length	Short-range energy
P-O_I	1.5337	$\psi_{PO}(1)$	Ca_{II}-F	2.297	ϕ_{CaF}	O_I-O_I	2.902	$\phi_{OO}(1)$
P-O_{III}	1.5342	$\psi_{PO}(2)$	Ca_{II}-O_{III}	2.349	$\phi_{CaO}(1)$	O_{II}-O_{III}	2.940	$\phi_{OO}(2)$
P-O_{II}	1.5406	$\psi_{PO}(3)$	Ca_{II}-O_{II}	2.371	$\phi_{CaO}(2)$	O_I-O_{III}	2.957	$\phi_{OO}(3)$
O_{III}-O_{III}	2.473	$\psi_{OO}(1)$	Ca_I-O_I	2.397	$\phi_{CaO}(3)$	O_{II}-O_{II}	3.013	$\phi_{OO}(4)$
O_{II}-O_{III}	2.487	$\psi_{OO}(2)$	Ca_I-O_{II}	2.452	$\phi_{CaO}(4)$	O_{II}-O_{III}	3.044	$\phi_{OO}(5)$
O_I-O_{III}	2.529	$\psi_{OO}(3)$	Ca_{II}-O_{III}	2.490	$\phi_{CaO}(5)$	O_{II}-O_{III}	3.208	$\phi_{OO}(6)$
O_I-O_{II}	2.538	$\psi_{OO}(4)$	Ca_{II}-O_I	2.684	$\phi_{CaO}(6)$	F-O_{III}	3.139	ϕ_{FO}
			Ca_I-O_{III}	2.801	$\phi_{CaO}(7)$			
			Ca_{II}-O_{III}	3.333	$\phi_{CaO}(8)$			

TABLE II. Solutions of the SEC for selected values of Z_O and $\psi'_{OO}(4)$ for the model in which short-range interactions are included for all pairs with bonds lengths < 2.81 Å. The ϕ' values do not depend on $\psi'_{OO}(4)$.

Z_O[a]	$\psi'_{PO}(1)$	$\psi'_{PO}(2)$	$\psi'_{PO}(3)$	$\psi'_{OO}(1)$	$\psi'_{OO}(2)$	$\psi'_{OO}(3)$	$\psi'_{OO}(4)$[a]	
−0.80	0.154	0.146	0.143	0.010	−0.048	−0.023	−0.100	
−1.15	−0.281	−0.249	−0.254	−0.061	−0.057	−0.054	−0.060	
−1.15	−0.183	−0.158	−0.162	−0.047	−0.093	−0.094	−0.100	
−1.50	−0.880	−0.836	−0.792	−0.164	−0.122	−0.148	−0.100	
	ϕ'_{CaF}	$\phi'_{CaO}(1)$	$\phi'_{CaO}(2)$	$\phi'_{CaO}(3)$	$\phi'_{CaO}(4)$	$\phi'_{CaO}(5)$	$\phi'_{CaO}(6)$	$\phi'_{CaO}(7)$
−0.80	−0.174	−0.080	−0.179	−0.143	−0.167	−0.091	−0.117	0.005
−1.15	−0.131	−0.130	−0.137	−0.156	−0.132	−0.091	−0.073	−0.027
−1.50	−0.082	−0.177	−0.088	−0.172	−0.098	−0.096	−0.037	−0.063

[a]Selected values.

solution on Z_O and $\psi'_{OO}(4)$ is shown by the results in Table II and Fig. 1, expressed in units where the electronic charge e and 1 Å are both taken as unity. *These units are employed throughout unless otherwise specified.* Since the nearly singular condition is due to forces within the PO_4^{-3} group the ϕ' values are independent of $\psi'_{OO}(4)$ to within at least ±0.0001, for wide ranging values of Z_O and $\psi'_{OO}(4)$.

The points on the graph in Fig. 1 are the values of ϕ'_{CaO} for $Z_O = -0.80$, -1.15, and -1.50 plotted as a function bond length. Notice that the $Z_O = -1.15$ values are relatively well behaved and approach zero whereas the $Z_O = -0.80$ and -1.50 values are quite scattered. On this basis alone, one would expect $Z_O \sim -1.15$ to be the more realistic value, and as we shall see, lattice-dynamical calculations bear this out as well.

Because of the well-behaved nature of the $Z_O \sim -1.15$ values it is possible to assume a Born–Mayer form for the Ca–O potential, $\phi_{CaO} = \lambda e^{-\alpha(r-r_0)}$, where r_0 can be any convenient value, and we choose $r_0 = 2.4$. This reduces the number of unknowns in ϕ'_{CaO} from seven to two and allows us to include the five ϕ'_{OO} forces. The resultant equations are nonlinear, but the solution is quickly obtained by an iterative procedure on the linear equations obtained by substituting the expanded form

$$\phi' = \phi'_0 + \left(\frac{\partial \phi'}{\partial \lambda}\right)_0 (\lambda - \lambda_0) + \left(\frac{\partial \phi'}{\partial \alpha}\right)_0 (\alpha - \alpha_0) \quad (1)$$

for the Ca-O forces. Typically, the solution is attained to within about ±0.0001 (for all ψ' and ϕ') after only two or three iterations when reasonable starting values are chosen. Reasonable estimates for λ_0 and α_0 may be obtained from a comparison of the points in Fig. 1 with curves of the form $\phi' = -\alpha\lambda e^{-\alpha(r-r_0)}$. The curve in Fig. 1 is for $\lambda = 0.0253$ and $\alpha = 4.24$, which are the values obtained for $Z_O = -1.15$. The dependence of the solutions on Z_O and $\psi'_{OO}(4)$ is illustrated by the results in Table III. As before, only the ψ' values depend on $\psi'_{OO}(4)$.

IV. VIBRATIONS OF THE FREE PHOSPHATE ION

The oxygen ions of a free PO_4^{-3} group lie at the corners of a tetrahedron while the P ion is at the center. The point symmetry group for this system is $\bar{4}3m$, and the group-theoretical reduction of the normal modes of vibrations is $A_1 + E + T_1 + 3T_2$. The T_1 "vibration" has zero frequency and corre-

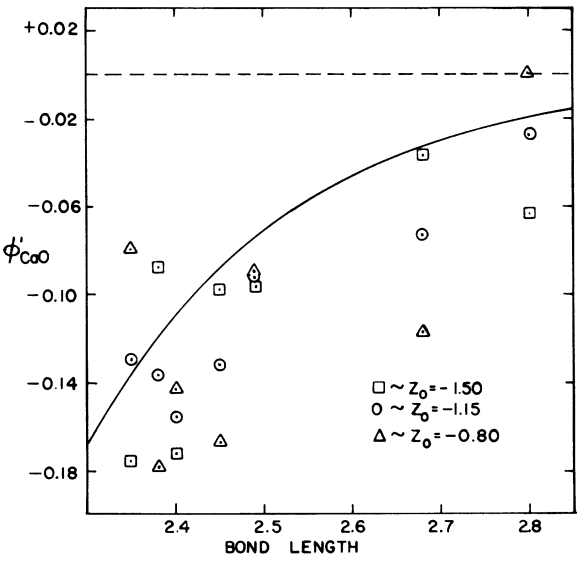

FIG. 1. Plot of the first derivative of the Ca–O short-range potentials as a function of bond length (units where the charge of the electron and 1 Å are unity). The points are for the model in which each Ca–O potential is treated separately while the curve is the Born–Mayer result for $Z_O = -1.15$.

TABLE III. Solutions of the SEC for selected values of Z_O and $\psi'_{OO}(4)$ for the model in which a Born–Mayer form, $\lambda e^{-\alpha(r-r_0)}$ with $r_0 = 2.4$, is used for the short-range part of the Ca-O interactions and those with bond lengths >3.07 are excluded. The ϕ' values and λ and α do not depend on $\psi'_{OO}(4)$.

Z_O[a]	$\psi'_{PO}(1)$	$\psi'_{PO}(2)$	$\psi'_{PO}(3)$	$\psi'_{OO}(1)$	$\psi'_{OO}(2)$	$\psi'_{OO}(3)$	$\psi'_{OO}(4)$[a]	
−1.10	−0.139	−0.116	−0.123	−0.116	−0.063	−0.096	−0.100	
−1.15	−0.191	−0.166	−0.170	−0.130	−0.091	−0.104	−0.100	
−1.15	−0.289	−0.257	−0.262	−0.094	−0.055	−0.065	−0.060	
−1.20	−0.235	−0.209	−0.209	−0.146	−0.127	−0.116	−0.100	
	ϕ'_{CaF}	λ	α	$\phi'_{OO}(1)$	$\phi'_{OO}(2)$	$\phi'_{OO}(3)$	$\phi'_{OO}(4)$	$\phi'_{OO}(5)$
−1.10	−0.106	0.0299	3.50	−0.061	−0.002	−0.039	−0.036	−0.012
−1.15	−0.112	0.0253	4.24	−0.049	−0.009	−0.034	−0.032	−0.016
−1.20	−0.121	0.0225	4.98	−0.031	−0.016	−0.023	−0.023	−0.024

[a]Selected values.

sponds to free rotations of the PO_4^{-3} group and similarly, one of the T_2 frequencies is zero owing to translational invariance. The real vibrations have frequencies $\nu_1 = 980$, $\nu_2 = 363$, $\nu_3 = 1082$, and $\nu_4 = 515$ in cm^{-1} and correspond, respectively, to the A_1, E, and the two T_2 modes.[6] Slightly different values have been quoted elsewhere.[7] All modes are Raman active and the two T_2 modes are also infrared active.

We write the potential energy Φ of the PO_4^{-3} group as a sum over all central pairwise interactions, i.e., $\Phi = 4\theta_{PO} + 6\theta_{OO}$, where $\theta_{PO}(\theta_{OO})$ is the total energy (Coulomb plus short range) of the P-O (O-O) pair. The static PO_4^{-3} group must be in equilibrium. This is accomplished by either requiring the force on the O ions in their equilibrium positions to be zero, or by minimizing the potential energy with respect to a uniform dilation. The condition for static equilibrium is $\theta'_{PO} = -\sqrt{6}\,\theta'_{OO}$, where, as before, the primes denote first derivatives with respect to bond length evaluated at the equilibrium separation. This is also the condition for rotational invariance in the harmonic approximation and hence, this condition causes the frequency of the T_1 "vibrations" to be zero.

One has, therefore, three adjustable parameters (the second derivatives, θ''_{PO} and θ''_{OO}, and say θ'_{PO}) for fitting to any three of the four frequencies. The masses, $m_P = 31$ and $m_O = 16$, in amu, are also needed for the calculation. Assuming that three-body potentials, which depend on the O–P–O angles, are the most important terms which we have omitted, the most reasonable choice is to fit to the ν_1, ν_3, and ν_4 vibrations, since these angles are most effected by the E modes. This is illustrated by the figure on p. 245 of Ref. 8. When the three adjustable parameters are so determined, the calculated ν_2 frequency is 333.0 cm^{-1}, lower than its measured value by only about 8%.

When the total potential energy is written as the sum of the Coulomb and short-range parts, the values of ν_1, ν_3, and ν_4 together with the condition $\theta'_{PO} = -\sqrt{6}\,\theta'_{OO}$, determine the short-range parameters ψ''_{PO}, ψ''_{OO}, ψ'_{PO}, and ψ'_{OO} in terms of Z_O and the P-O bond length. Taking this distance to be the average of the crystal values (1.536) the dependence on Z_O is shown in Table IV. These values provide rough estimates for the ψ''_{PO}, ψ''_{OO}, and $\psi'_{OO}(4)$ crystalline values.

TABLE IV. Values of the short-range parameters for free PO_4^{-3} vibrations as a function of Z_O.

Z_O	ψ''_{PO}	ψ''_{OO}	ψ'_{PO}	ψ'_{OO}
−1.10	3.42	0.186	0.047	−0.093
−1.15	3.59	0.171	−0.081	−0.075
−1.20	3.76	0.157	−0.216	−0.057

V. LATTICE DYNAMICS OF FLUORAPATITE FOR ZERO WAVE VECTOR

The Coulomb part of the dynamical matrix for wave vector $\vec{q}$ is not single valued in the limit as $\vec{q} \to 0$ but depends on the direction of $\vec{q}$. The nonregular part, which affects the infrared active modes, may be expressed in terms of macroscopic electric field oscillations that accompany the long-

TABLE V. Multiplicities due to site symmetries a, f, h, and i in space group $P6_3/m$, and the total multiplicities for the FAP structure.

Occupied site symmetries (Wyckoff notation)	Irreducible representations A_g	B_g	E_{1g}	E_{2g}	A_u	B_u	E_{1u}	E_{1u}
a	0	1	0	1	1	0	1	0
f	1	1	1	1	1	1	1	1
h	2	1	1	2	1	2	2	1
i	3	3	3	3	3	3	3	3
Total	12	9	8	13	9	12	13	8

wavelength vibrations (see Paper I). Zero-wave-vector dynamics refers to the long-wavelength dynamical problem with the nonregular part omitted, and this is the problem we consider here. Since FAP has inversion symmetry the Raman and infrared active modes are completely decoupled and hence the Raman active modes are not affected by the nonregular part.

The $\vec{q}=0$ dynamical matrix and the matrix which group theoretically block diagonalizes it were constructed by the computer using the general formulas discussed in Paper I. The number of modes (multiplicity) for each symmetry is listed in Table V, where the symbols A_g, B_g, etc., identify the symmetry of the modes with the irreducible representations of the point group $6/m(C_{6h})$. The A and B modes are singly degenerate while the E modes are doubly degenerate. The total multiplicity is the sum of the contributions for each set of nonidentical ions and two sets with the same site symmetry contribute the same to the total. There are 33 Raman active modes $(12A_g+8E_{1g}+13E_{2g})$ and 20 that are infrared active $(8A_u+12E_{1u})$. The number of infrared active modes for both A_u and E_{1u} is one less than the total multiplicity since the zero-frequency acoustic modes have these symmetries.

The dynamical matrix is computed from the mass and charge of the ions, the crystal structure, and the first and second derivatives of the short-range potentials. The structure is given in Ref. 5 and the masses are $m_F=19$, $m_{Ca}=40$, $m_P=31$, and $m_O=16$, in amu. The fully ionic values are taken for the charge of the F, Ca, and PO_4 ions while the charge on the oxygens, Z_O, is adjustable. We use the model, described in Sec. III, in which a Born–Mayer form is chosen for the Ca-O interactions.

The frequencies of the Raman active modes for two models with $Z_O=-1.10$ and -1.15 are shown in Fig. 2 for comparison with the Raman spectra. The scattering geometries $z(xz)y$, $y(zz)x$, and $z(yx)y$ are such that only E_{1g}, A_g, and E_{2g} modes, respectively, are excited.[8] Values for those first and second derivatives of the short-range interactions, which are not already given by the results in Table III, are listed in Table VI. Six adjustable parameters (not including Z_O) were determined by fitting to those frequencies so indicated in Fig. 2. We postpone for the moment the detailed description of the adjustable parameters and precisely how they were obtained and discuss now the correlation between experiment and theory.

For convenience, let $A_g(i)$ refer to the ith mode with A_g symmetry where $A_g(1)$ is the lowest-frequency mode, $A_g(2)$ the second-lowest, etc., and similarly for the other symmetries. The frequencies of all modes for the $Z_O=-1.10$ model are shown in Fig. 3, where they are classified according to their symmetries (left) and whether they correspond to lattice modes or particular modes of the free PO_4^{-3} ion (top). There are six PO_4^{-3} ions per unit cell, and since the A_1 mode for the free ion is singly degenerate, there are six such modes in the lattice (E modes are doubly degenerate). Similarly 18 modes correspond to each of the T_2 free-ion vibrations since they are triply degenerate in the free ion and 12 correspond to the doubly degenerate E mode of the free ion. The $T_2(\nu_3)$ vibrations are on the average shifted down by about 15 cm^{-1} from their free-ion value of 1082 cm^{-1} and the $A_1(\nu_1)$ modes are similarly shifted by 25 cm^{-1} from 980 cm^{-1}. On the other hand, the $T_2(\nu_4)$ and $E(\nu_2)$ modes are shifted to higher frequencies by average amounts of 65 and 80 cm^{-1} from their free-ion values of 515 and 333 cm^{-1}.[9] Except for the $A_1(\nu_1)$ modes the frequencies of these vibrations are scattered over a considerably wider range for the u-symmetry vibrations.

There are two features of the measured spectrum which at first *appear* to spoil the generally very good correlation between experiment and theory shown in Fig. 2. The peak at 960 cm^{-1} in the $z(xz)y$ geometry is not an E_{1g} phonon but a leak of the very intense peak in $y(zz)x$ into this geometry, resulting from the finite solid angle of the collection optics. Also, the weak peak at 1025 cm^{-1} in $y(zz)x$ is almost certainly not a phonon for two reasons. First of all, from the theory, it is simply not possible to have four A_g phonons with frequencies in the range 950–1100 cm^{-1} without using completely ridiculous values for some of the force constants and at the same time destroying the rest of the good correlation. Secondly, the peak was not mentioned by Kravitz *et al.*[10] in their report of similar measurements on fluorapatite. Another unexplained feature of the spectrum is the appearance of a small low-frequency shoulder in the $x(yx)y$ geometry on the $E_{2g}(8)$ line. The strength of this feature is approximately 10% of the $E_{2g}(8)$ phonon and its frequency is shifted by about 10 cm^{-1}. This is not seen in the $z(yx)y$ geometry [Fig. 2(c)] which theoretically should detect the same phonons as $x(yx)y$.

The greatest real discrepancy between the calculations and observations is that the frequencies of $A_g(7)$, $E_{1g}(6)$, and $E_{2g}(8)$ are approximately 50 cm^{-1} too low. However, we expect them to be 30 cm^{-1} too low since they correspond to the $E(\nu_2)$ vibrations of the free phosphate ion, and we are neglecting angle-bending forces (see Sec. IV). The remaining frequencies ($Z_O=-1.10$) match nicely with their measured values to within about 25 cm^{-1} in all cases and suggest that the peaks at 160 and 310 cm^{-1} in $y(zz)x$ are both really unresolved double peaks. When Z_O is decreased from the best

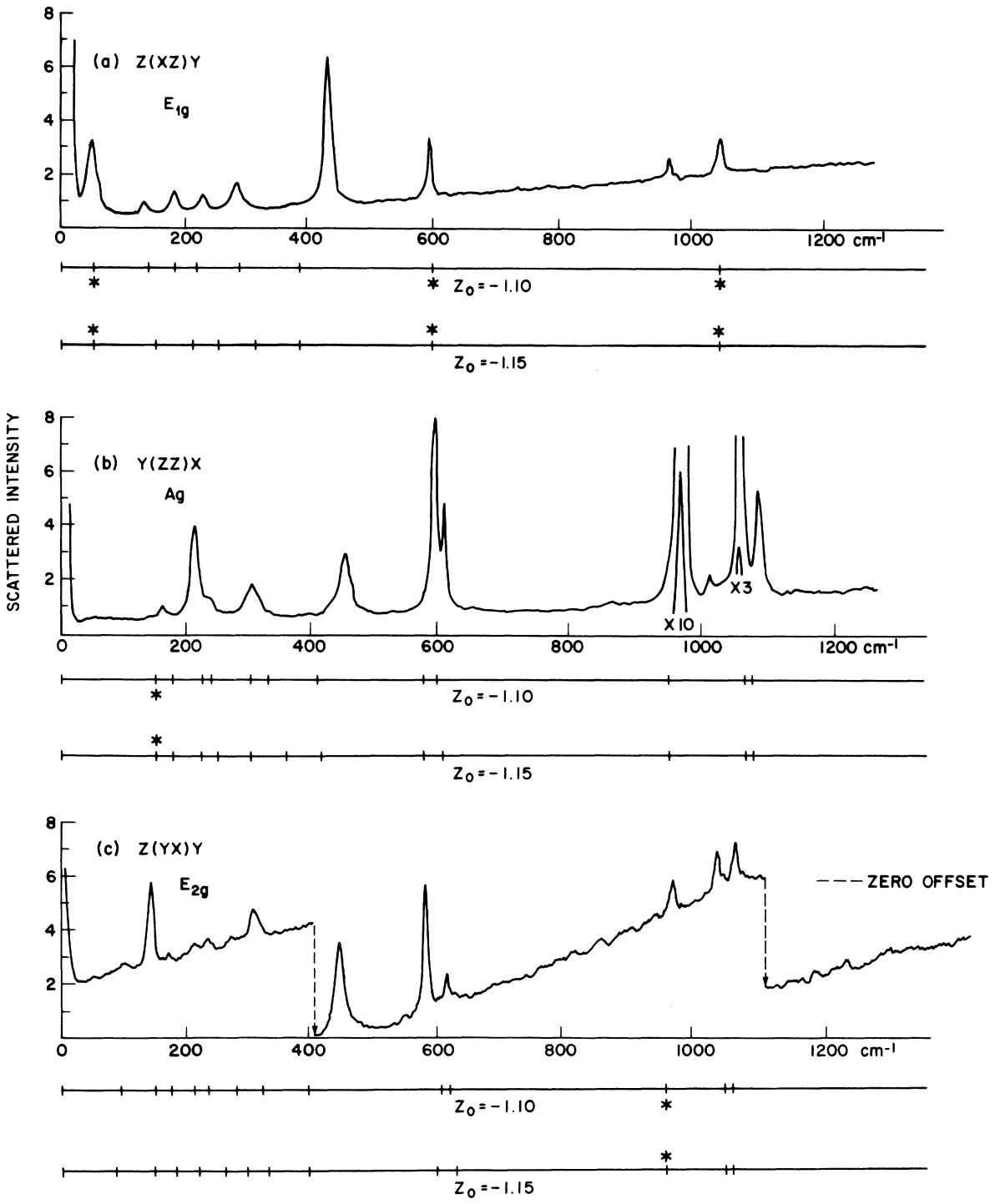

FIG. 2. Raman spectra for $y(zz)x$, $y(zy)x$, and $z(yx)y$ geometries and computed frequencies of the A_g, E_{1g}, and E_{2g} modes for two values, -1.10 and -1.15, of Z_O. The frequencies of the Raman lines are indicated in cm^{-1}. Fitted frequencies are indicated by asterisks.

value of -1.10 to -1.15 some of the lattice modes are shifted to frequencies that are considerably too high, thus tending to spoil the good correlation.

There are three additional doublets in the $y(zz)x$ spectrum at 225, 600, and 1065 cm^{-1} that are resolved. A possible explanation of this proclivity

TABLE VI. Values for some of the first and second derivatives of short-range interactions used in the calculations in Fig. 2. $\psi''_{PO} \equiv \psi''_{PO}(1) = \psi''_{PO}(2) = \psi''_{PO}(3)$ and similarly for ψ''_{OO} and ϕ''_{OO}. Values not listed here are given by the results in Table III. The units are such that $e = 1$ and 1 Å = 1.

Z_O	ψ''_{PO}	ψ''_{OO}	ϕ''_{CaF}	ϕ''_{OO}	ϕ''_{FO}		
−1.10	3.217	0.100	0.400	0.090	0.102		
−1.15	3.391	0.073	0.390	0.061	0.117		
Z_O	$\psi'_{PO}(1)$	$\psi'_{PO}(2)$	$\psi'_{PO}(3)$	$\psi'_{OO}(1)$	$\psi'_{OO}(2)$	$\psi'_{OO}(3)$	$\psi'_{OO}(4)$
−1.10	0.197	0.193	0.189	−0.238	−0.187	−0.232	−0.237
−1.15	0.035	0.042	0.040	−0.212	−0.174	−0.195	−0.192

for double peaks can be found in the crystal structure. The apatite structure is actually a distortion from a higher-symmetry structure having space group $P6_3/mcm$.[11] There are 6 A_{1g} and 6 A_{2g} phonons in the high-symmetry structure which combine to give the 12 A_g modes in the apatite structure. The A_{1g} phonons are Raman active while those with A_{2g} symmetry are not. The natural conclusion is that the weakest of each doublet and the peak at 460 cm^{-1} are associated with the A_{2g} phonons while the strongest of the pairs and the very intense 960-cm^{-1} peak correspond to the Raman active A_{1g} modes.

Infrared reflectance spectra have been measured by Kravitz *et al.*[10] for $\nu > 300$ cm^{-1}. They find resonant frequencies at 1070, 565, and 310 cm^{-1} due to A_u phonons and at 1110, 1060, 610, 575 and 335 cm^{-1} due to E_{1u} phonons. These correspond to our calculated frequencies (Fig. 3) for the $A_u(8)$, $A_u(7)$, $A_u(5)$, $E_{1u}(12)$, $E_{1u}(11)$, $E_{1u}(9)$, $E_{1u}(8)$, and $E_{1u}(6)$ modes to within 30 cm^{-1} in all cases. As the $A_u(6)$, $E_{1u}(10)$, and $E_{1u}(7)$ modes correspond to free PO_4^{-3} vibrations which are not infrared active they are expected to be only weakly infrared active in the lattice and consequently they do not show up in the reflectance spectra.

The adjustable parameters, i.e., those not determined by the static-equilibrium conditions, are ψ''_{PO}, ψ''_{OO}, ϕ''_{CaF}, ϕ''_{OO}, ϕ''_{FO}, $\psi'_{OO}(4)$, and Z_O. As the three P-O interactions have nearly the same bond length we assume identical values for their second derivatives, that is, $\psi''_{PO} \equiv \psi''_{PO}(1) = \psi''_{PO}(2) = \psi''_{PO}(3)$, and similarly for ψ''_{OO} and ϕ''_{OO}. For reasons discussed below, we allow ϕ''_{FO} to take on nonzero values even though ϕ'_{FO} is assumed to be zero. The best value for Z_O is obtained by simply inspecting the computed Raman frequencies for an overall correlation with the measured values, as illustrated in Fig. 2. The remaining six parameters are determined by fitting to specific features of the Raman spectrum.

One first constructs an approximate model in which reasonable estimates of the adjustable parameters are obtained from the static-equilibrium conditions and the dynamics of the free PO_4^{-3} ion. The latter provides approximate values for ψ''_{PO}, ψ''_{OO}, and $\psi'_{OO}(4)$. The value of ϕ''_{CaF} was initially assumed to be that of the nearest Ca-O interaction, and this is given by the Born–Mayer parameters. Similarly, the value of ϕ''_{OO} was expected to be approximately the same as $\phi''_{CaO}(7)$. Initially ϕ''_{FO} was taken to be zero while the results in Fig. 1

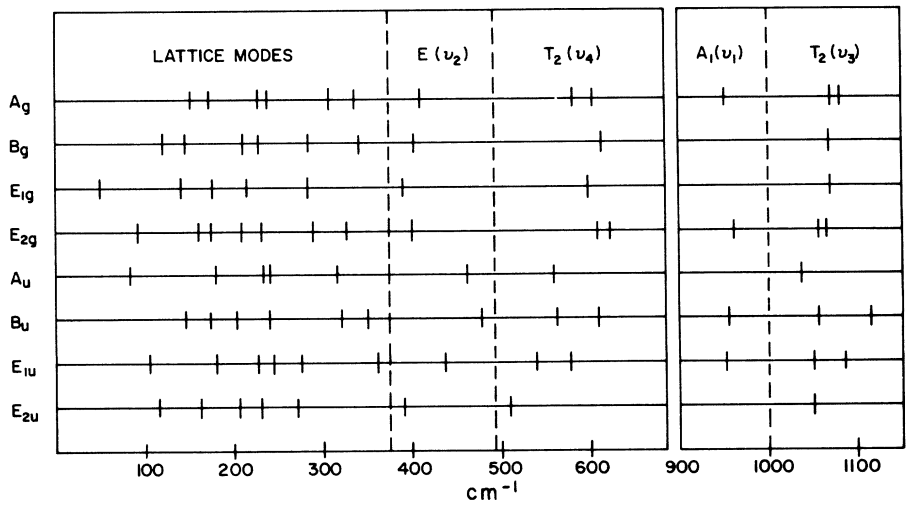

FIG. 3. Frequencies of all zero-wave-vector phonons for the $Z_O = -1.10$ model classified according to their symmetries (left) and whether they correspond to lattice modes or vibrations of free PO_4^{-3} ions (top).

suggested that $Z_O \sim -1.15$.

For such approximate models it is possible to identify most of the appropriate computed frequencies with specific lines in the Raman spectrum. Once the identification is made the model is then refined to improve the correlation. The partial derivatives of the fitted frequencies (Fig. 2) with respect to the adjustable parameters (excluding Z_O) were determined numerically. They are the coefficients in a set of six linear equations in these unknowns which are then solved in an iterative fashion for the values required to fit the measured ones.

Some discretion must be exercised, of course, in deciding which frequencies should be fitted. As a general rule, one should determine the parameters from the modes that are most affected by them. Clearly, those modes which correspond to the ν_1, ν_3, and ν_4 vibrations of the free phosphate ion are strongly affected by ψ''_{PO}, ψ''_{OO}, and $\psi'_{OO}(4)$, and thus, these parameters are determined primarily from the three highest-frequency fitted values. The frequency of $E_{1g}(1)$, which for the approximate model was considerably too low, was found to be strongly dependent on $\psi''_{CaO}(7)$ and ϕ''_{FO}, and only these parameters. Rather than change $\phi''_{CaO}(7)$ from its Born–Mayer value, ϕ''_{FO} was determined on this basis. Similarly, $A_g(1)$ was fitted since it depends rather strongly on ϕ''_{OO}. The $E_{2g}(8)$ mode is quite strongly affected by ϕ''_{CaF} in comparison to its effect on $A_g(7)$ and $E_{1g}(6)$. These modes correspond to the $E(\nu_2)$ vibrations of free PO_4^{-3} and have frequencies which are naturally too low because of our neglect of angle-bending forces. Therefore it is not realistic to fit $E_{2g}(8)$ to the measured value, so its frequency was instead chosen to be half way between the computed values for $E_{1g}(6)$ and $A_g(7)$, in agreement with the measured spectrum.

From the results in Fig. 2, some of the lattice-mode frequencies are apparently quite sensitive to the value of Z_O. On the other hand, this effect is primarily due to the change in the Born–Mayer parameters that results from the static-equilibrium conditions rather than from the change in the Coulomb part of the dynamical matrix. In other words, one should not be precise in judging the "true" value of Z_O on this basis since the best value for this model may to some extent be due to the Born–Mayer approximation of the Ca-O potentials. In fact, similar calculations using the first model discussed in Sec. III (short-range potentials with the bond lengths greater than 2.81 Å excluded) resulted in rather good agreement with experiment, but over wider ranging values of Z_O. For this model the seven ϕ''_{CaO} values, as well as those for ψ''_{PO}, ψ''_{OO}, ϕ''_{CaF}, and $\psi'_{OO}(4)$, were all determined by fitting measured frequencies. While good agreement was obtained for several values of Z_O ranging from -1.10 to -1.30 the resulting values of ϕ''_{CaO}, when plotted as a function of bond length, were less well behaved as Z_O moved away from circa -1.15. The main deficiency of this latter model is that the frequencies of the modes corresponding to $E(\nu_2)$ of the free PO_4^{-3} are about 25 cm^{-1} lower than those for the previous model. These modes are stiffened to the values shown in Fig. 2 primarily by the ϕ_{OO} interactions, and this points out the need for including them in the model.

The best value which we obtain for Z_O is also a consequence of our neglect of polarization. The oxygen ions are the most polarizable and are likely in sites of high local field. By taking an adjustable charge on the oxygens we are free to adjust the electric field due to these ions and thus, to some extent, correct for our neglect of their dipole terms. In two separate quantum-mechanical calculations for the free PO_4^{-3} ion McAloon and Perkins[12] obtained values of -1.02 and -0.65 for Z_O. The latter value is expected to be the better of the two since more orbitals were included in its computation. The effect of including dipole terms in the oxygen charge distribution would presumably be an increase in our best value of Z_O to a value in closer agreement with the quantum-mechanical calculations. On the other hand, judging from the generally very good agreement that we obtain with Raman and infrared data, the adjustable Z_O seems to compensate rather well for this neglect.

---

*Work at Princeton supported by Grant No. DE02492 of the National Institute of Health.

†Present address: Code 6440, Naval Research Laboratory, Washington, D. C. 20375.

[1]L. L. Boyer, preceding paper, Phys. Rev. B 9, 2684 (1974).

[2]For a review, see *Structural Properties of Hydroxyapatite and Related Compounds*, edited by W. E. Brown and R. A. Young (Gordon and Breach, to be published).

[3]D. M. Roy, Mater. Res. Bull. 6, 1337 (1971).

[4]M. Mengeot, M. L. Harvill, and O. R. Gilliam (private communication).

[5]K. Sudarsanan, P. E. Mackie, and R. A. Young, Mater. Res. Bull. 7, 1331 (1972).

[6]G. Herzberg, *Molecular Spectra and Molecular Structure. II. Infrared and Raman Spectra of Polyatomic Molecules* (Van Nostrand, Princeton, 1945) p. 167.

[7]*Topics in Phosphorous Chemistry*, edited by M. Grayson and E. J. Griffith (Wiley, New York, 1969), Vol. 6, p. 326.

[8]R. Loudon, Advan. Phys. 13, 423 (1964).

[9]The value 333 cm^{-1} for $E(\nu_2)$ is not the measured value but calculated as described in Sec. IV.

[10]L. C. Kravitz, J. D. Kingsley, and E. L. Elkin, J. Chem. Phys. 49, 4600 (1968).

[11]L. L. Boyer, Phys. Status Solidi A 20, 555 (1973).

[12]B. J. McAloon and P. G. Perkins, Theor. Chem. Acta 22, 304 (1971).